FINITE ELEMENT MODELING OF CONCRETE MASONRY-INFILLED STEEL FRAMES

W. El-Dakhakhni[1] , M. Elgaaly[2] , and A. Hamid[3]

ABSTRACT

Masonry infilled panels in framed structures have been long known to affect strength, stiffness and ductility of the composite structure. In seismic areas, however, ignoring the composite action is not always on the safe side, since the interaction between the panel and the frame under lateral loads dramatically changes the stiffness and the dynamic characteristics of the composite structure and hence its response to seismic loads. This study presents a simple practical method of estimating the stiffness and the lateral load capacity of concrete masonry-infilled steel frames (CMISF) failing in corner crushing (CC) mode, as well as the internal forces in the steel frame members using finite element method (FEM) analysis. In this method, each masonry panel is replaced by three struts with force-deformation characteristics based on the orthotropic behavior of the masonry infill. A simplified steel frame model is also presented based on the documented modes of failure of CMISF. The method can be easily computerized and included in the analysis and design of three-dimensional CMISF structures. The proposed technique accounts for the non-linear behavior that occur in the steel frame due to formation of plastic hinges, and in the masonry panel due to crushing. It has been demonstrated that the proposed model can predict both the stiffness and the ultimate lateral load capacity of such systems.

Key Words: Concrete Masonry, FEM Modeling, Infilled Steel Frames, Orthotropic Masonry, Three Strut Model.

[1] Research Assistant, Department of Civil and Architectural Engineering, Drexel University, Philadelphia, PA, 19104, USA. E-mail : wwe22@drexel.edu
[2] Professor, Department of Civil and Architectural Engineering, Drexel University, Philadelphia, PA, 19104, USA. E-mail : elgaalym@drexel.edu
[3] Professor, Department of Civil and Architectural Engineering, Drexel University, Philadelphia, PA, 19104, USA. E-mail : hamidaa@drexel.edu

INTRODUCTION

Masonry infilled panels can be found as interior and exterior walls in reinforced concrete and steel framed structures. Since they are normally considered as architectural elements, their presence is often ignored by structural engineers. However, they tend to interact with the surrounding frame when the structure is subjected to strong earthquake loads; the resulting system is referred to as an *infilled frame*. Ignoring the effect of the infill in stiffening and strengthening the surrounding frame is not always a conservative approach, since the stiffer the building, usually, the higher seismic loads it attracts. If the panel is overstressed and hence failed partially or wholly, the high forces previously attracted and carried by the stiff infilled frame, will be suddenly transferred to *the more flexible* frame after the infill is partially or fully damaged. In addition, change in stiffness distribution can result in higher seismic forces due to torsional effects. Because of the complexity of the problem and the absence of a realistic, yet simple analytical model, the effect of masonry infill panels is often neglected in the nonlinear analysis of building structures. Such an assumption may lead to substantial inaccuracy in predicting the lateral stiffness, strength, and ductility of the structure. It will also lead to uneconomical design of the frame since the strength and stiffness demand on the frame could be largely reduced. The current study aims to present a simple method of predicting the stiffness as well as the ultimate load capacity of concrete masonry-infilled steel frames (CMISF). The method can be used to produce design aids and to develop a conceptual approach of analysis and design of such systems.

FAILURE MODES OF INFILLED FRAMES

Based on the knowledge gained from the research work during the last five decades, failure modes of masonry infilled frames can be categorized into five distinct modes, namely:
1. Corner crushing mode (*CC mode*), represents crushing of the infill in at least one of its loaded corners, as shown in Fig. 1-a. This mode is usually associated with infill of weak masonry blocks surrounded by a frame with weak joints and strong members.
2. Sliding shear mode (*SS mode*), represents horizontal sliding shear failure through bed joints of a masonry infill, as shown in Fig. 1-b. This mode is associated with infill of weak mortar joints and strong frame.
3. Diagonal compression mode (*DC mode*), represents crushing of the infill within its central region, as shown in Fig. 1-c. This mode is associated with a relatively slender infill, where failure results from out-of-plane buckling instability of the infill.
4. Diagonal cracking mode (*DK mode*), in the form of a crack connecting the two loaded corners, as shown in Fig. 1-d. This mode is associated with weak frame or frame with weak joints and strong members infilled with a rather strong infill.
5. Frame failure mode (*FF mode*), in the form of plastic hinges in the columns or the beam-column connection, as shown in Fig. 1-e. This mode is also associated with weak frame or frame with weak joints and strong members infilled with a rather strong infill.

It is worth mentioning that only the first two modes are of practical importance, since the third mode is very rare to occur and requires a high slenderness ratio of the infill to result in

out-of-plane buckling of the infill under *in-plane* loading, this is hardly the case when practical panel dimensions are used. The fourth mode should not be considered a failure mode because the infill can still carry more load after it cracks. The fifth mode should be considered in the case of RC frames, but for *steel* frames infilled with *unreinforced hollow concrete* masonry blocks, this mode hardly occurs. The study conducted herein models the *CC* mode only, which is the most common mode of failure for CMISF.

DEVELOPMENT OF CMISF MODEL

Subjecting a *bare* masonry panel to a diagonal loading results in a sudden failure because of *unconfinement*. This failure is usually initiated by a stepped crack along the loaded diagonal, dividing the panel into two separate parts. This behavior was investigated by ElDakhakhni (2000) using ANSYS®5.3 FE program. The *ASTM E-519* diagonal tension test specimen, representing this loading case, and the FE model used to duplicate the experimental failure mechanism are both shown in Fig. 2. Unlike the unconfined panel, as soon as a diagonal crack develops within an infilled panel (usually at a much lower load and deflection levels than ultimate) the panel finds itself confined within the surrounding frame and bearing against it over *contact lengths*, as shown in Fig. 3. The contact lengths provide enough confinement to prevent failure and allows the panel to carry more load until existing diagonal crack continues to widen and new cracks appears leading, *eventually*, to ultimate failure. This behavior was repeatedly reported in the literature by many researchers [Polyakov (1956), Stafford-Smith and Carter (1969), Flanagan et al. (1992), Saneinejad and Hobbs (1995) and Seah (1998)].

From the above discussion it is more rational to consider the panel to be composed of *two diagonal regions* as shown in Fig. 3, one connecting the top beam to the leeward column and the other connecting the windward column to the lower beam. From a different aspect, as reported by many researchers, [Reflak and Fajfar (1991), Saneinejad and Hobbs (1995) , Mosalam et al. (1997a,b,c), Buonopane and White (1999), and Furutani et al. (2000)], the bending moments and shearing forces in the frame members cannot be replicated using a *single diagonal* strut connecting the two loaded corners. Based on the above, it is suggested that, at least *two* additional *off-diagonal* struts located at the points of maximum field moments in the beams and the columns are required to reproduce these moments as shown in Fig.3. Furthermore, since the interaction between frame members and the infill depends on the contact length which, in turn, is affected by the stiffness and the deflected shape of the frame members, the use of a multi-strut model will allow for the *interaction* between different panels in multi-story buildings. This is due to the fact that some beams (and/or columns) will be loaded from the upper and lower panels (or left and right panels) at different locations within the span (or height), which will affect their deflected shape and hence the panel's strains, and consequently changing the failure load. Using the ANSYS®5.3 FE program, ElDakhakhni (2000) modeled a single panel infilled frame using PLANE42 plane stress elements connected to the frame BEAM3 elements with CONTACT12 contact elements. The stressed part of the panel, as shown in Fig. 4, is in the form of a diagonal *area*. The use of multi-strut model rather than a single strut will better represent the actual stressed

area within the infill, and will also facilitate the modeling of the *progressive* failure occurring at the corners contact *region*, not just at the corner *points*.
The development of the infilled frame analytical model is divided into two parts. The first part deals with the development of a FE model for the *geometrical* representation of the structural system's components, namely, the steel frame and the infill panel. The second part deals with the *material* model suggested for these two components.

STEEL FRAME GEOMETRICAL MODEL

The steel frame members were modeled with ANSYS®5.3 FE program using BEAM3, an *elastic* beam elements connected by *non-linear rotational* spring elements, COMBIN39, at the beam-column joints. The *concentration* of *non-linearity* in the frame joints *only*, is based on the fact that due to the limited infill ductility and thus limited frame deformation at the peak load except at the loaded corners, the maximum field moments as well as the bending moments at the unloaded joints are lower than that at the loaded joints and has been found to be, *at most*, 20% of the plastic moment capacity of the section [Saneinejad and Hobbs (1995)]. Unlike the model suggested by Seah (1998), which allows for the interaction between the axial and shear forces and the bending moment at the connection, no *translational* springs were used at the joint of the suggested model, instead, the DOF *coupling* option provided in ANSYS®5.3 was used to couple both the beam and the column nodes at the beam-column connection in the two planer translational DOF and forced them to undergo the same displacement.

INFILL PANEL GEOMETRICAL MODEL

Saneinejad and Hobbs (1995) showed that for steel frame members infilled with *plane concrete* panel, the points of maximum field moment developed within the frame members lie approximately at the end of the contact lengths, and are located at distances from the beam-column connection given by

$$\alpha_c h = \sqrt{\frac{2\,(M_{pj} + \beta_c M_{pc})}{\sigma_c t}} \le 0.4h \qquad \alpha_b l = \sqrt{\frac{2\,(M_{pj} + \beta_b M_{pb})}{\sigma_b t}} \le 0.4l \qquad \text{(1-a,b)}$$

where, α_c is the ratio of the column contact length to the height of the column and α_b is the ratio of the beam contact length to the span of the beam; h is the column height and l is the beam span. M_{pj} is the minimum of the column's, the beam's or the connection's plastic moment capacity, referred to as the plastic moment capacity of the joint; M_{pc} and M_{pb} are the column and the beam plastic moment capacities, respectively; σ_c and σ_b are the normal contact stresses on the face of the column and the beam, respectively; β_c and β_b are the ratios between the maximum elastic field moment developed within the height of the column to M_{pc} and that developed within the span of the beam to M_{pb} respectively; and finally t is the thickness of the panel.
It is worth mentioning that these contact lengths are not constant and they vary throughout the loading history. Saneinejad and Hobbs (1995) suggested that, near failure, either σ_c and β_c

or σ_b and β_b will reach their respective upper bound values of σ_{co} and β_o or σ_{bo} and β_o, depending on whether the infill failure is initiated on the column's or the beam's face respectively. They suggested a method to determine σ_c and σ_b , and demonstrated, based on FEM analysis, that β_0=0.2. For simplicity, and assuming full crushing of the infill in the loaded corners region near failure, it is suggested that β_c, β_b, σ_c , and σ_b have reached their respective upper bound values. The upper bound values of σ_c and σ_b , namely σ_{co} and σ_{bo}, suggested by Saneinejad and Hobbs (1995) are given by

$$\sigma_{co} = \frac{f'_c}{\sqrt{1 + 3\ \mu^2 r^4}} \qquad \sigma_{bo} = \frac{f'_c}{\sqrt{1 + 3\ \mu^2}} \qquad \text{(2-a,b)}$$

where, f'_c is the compressive strength of the *plane concrete* panel; and μ is the coefficient of friction between the steel frame and the concrete panel; and r is the panel's aspect ratio defined as $r = h/l < 1$. In order to modify the above equations to suit the concrete masonry, f'_c should be replaced by $f'_{m\text{-}0}$ and $f'_{m\text{-}90}$ in equations 2-a and 2-b, respectively, where $f'_{m\text{-}0}$ and $f'_{m\text{-}90}$ are the compressive strength of the masonry panel parallel and normal to the bed joint respectively; since, unlike the isotropic plane concrete, concrete masonry is anisotropic or, at best, orthotropic. Furthermore, since μ between steel and masonry is small (usually about 0.3), and the shrinkage of the concrete infill may result in a separation between the frame and the panel; a rational assumption will be to neglect the friction between the steel frame and the masonry. A similar assumption was also suggested by Liauw and Kwan (1982) assuming friction to be a strength reserve. It is also worth mentioning that a recent study conducted by Flanagan et al. (1999) concluded that the method suggested by Saneinejad and Hobbs (1995) estimated twice the capacity obtained from experimental work that the best results were obtained with $\mu = 0$. Also since $r < 1$, then r^4 is very small and can be neglected.

Summarizing the above assumptions and simplifications, it is suggested that the distances from the beam column connection to the points of maximum field moments in the frame columns and beams (which are also approximately the contact lengths) are to be given by equations 5 and 6, respectively,

$$\alpha_c h = \sqrt{\frac{2\ (M_{pj} + 0.2\ M_{pc})}{t\ f'_{m-0}}} \le 0.4h \qquad \alpha_b l = \sqrt{\frac{2\ (M_{pj} + 0.2\ M_{pb})}{t\ f'_{m-90}}} \le 0.4l \qquad \text{(3-a,b)}$$

Referring to Fig. 3 it is more practical to use strut instead of plate elements to represent the two regions of the panel. Assuming that the equivalent uniformly loaded diagonal region of the panel to be of area equal to A, where A is to be determined later, hence each region of the panel shown in Fig. 3 will be of area $=A/2$. Furthermore, assuming uniform contact stress distribution along the contact areas, each region will be replaced by two struts, each of area $A_1=1/2\times(A/2)=A/4$, located at the beginning and the end of the contact length. Combining the two struts connecting the loaded corners, from the two regions, into one strut of area $A_2 = 2\times A_1 = A/2$ results in representing the whole panel by three struts, an upper strut connecting the upper beam with the leeward column with area $A_1=A/4$, a middle strut connecting the two loaded corners with area $A_2=A/2$, and finally a lower strut of area $A_1=A/4$ connecting the windward column with the lower beam, where $A=2A_1+A_2$. A diagram showing the proposed geometrical model for a typical CMISF is shown in Fig. 5.

Saneinejad and Hobbs (1995) replaced the panel by a single strut with an area A_d given by

$$A_d = \frac{(1-\alpha_c)\alpha_c h\ t\ \frac{\sigma_c}{f_c} + \alpha_b l\ t\ \frac{\tau_b}{f_c}}{\cos\theta} \tag{4}$$

where, f_c is a *reduced* strength for the concrete to account for the ultimate design limit state; θ is defined as $\tan^{-1}\theta = (h/l)$; and τ_b is an equivalent uniform shear stress developed on the beam-infill interface and is defined as $\tau_b = \mu\ \sigma_b$. Again based on the previous discussion, it is suggested to neglected the τ_b term in equation 4. Furthermore, since this study deals with the behavior of infilled frames up to *failure*, no material reduction factor will be employed. Then f_c will be assumed to reach its upper bound value for masonry parallel to bed joint of $f'_{m\text{-}0}$. At failure, referring to the discussion following equations 2-a and 2-b, σ_c will also reach its upper bound value of σ_{co} which is, for concrete masonry, approximately equal to $f'_{m\text{-}0}$. This will result in reducing the f_c/σ_{co} factor to unity. In this assumption, the effect of the biaxial state of stress in the infill corners vicinity was neglected for simplicity. Based on the above, it is suggested that the total diagonal struts area, *A*, is to be calculated by

$$A = \frac{(1-\alpha_c)\alpha_c h\ t}{\cos\theta} \tag{5}$$

STEEL FRAME MATERIAL MODEL

The ultimate moment capacity of the non-linear rotational spring, representing the beam-column joint, is defined as the minimum of the column's, the beam's or the connection's ultimate capacity, M_{pj}, which will be referred to as the plastic moment capacity of the joint, as defined earlier in equations 1 and 2. The *rotational stiffness* of the spring can be calibrated so that the *lateral stiffness* of the frame model matches that of the actual bare frame, which can be obtained experimentally or using simple elastic analysis or, in case of semi-rigidly connected members, using available data on modeling semi-rigid connections [Chen and Lui (1991)]. The joint behavior is shown in Fig. 5, where, ϕ_{el} is the maximum elastic rotation that the joint can undergo without yielding; ϕ_{pl} is the maximum plastic rotation before the joint undergoes moment reduction below M_{pj}; and ϕ_{ult} is the maximum plastic rotation beyond which the joint cannot sustain any moment.

INFILL PANEL MATERIAL MODEL

Based on the available literature, it is evident that the stressed part of the panel is a diagonal region connecting the two loaded corners. It is therefore justifiable to assume that the panel properties in the diagonal direction are the properties governing the behavior of the infill panel. Masonry panels have been known to be anisotropic, [Hamid and Drysdale (1980), Khattab and Drysdale (1992), Mosalam et al. (1997c) and Seah (1998)]. A close approximation is to consider the anisotropic masonry panel to be orthotropic. Due to the fact that the panel behaves as if it was *diagonally loaded*, constitutive relations, of orthotropic

plates [(Shames and Cozzarelli (1992)] and axes transformation matrix, are used to obtain the Young's modulus, E_θ, of the panel in the diagonal direction using the following equation

$$E_\theta = \frac{1}{\frac{1}{E_0}\cos^4\theta + \left[-\frac{2\nu_{0-90}}{E_0} + \frac{1}{G}\right]\cos^2\theta\sin^2\theta + \frac{1}{E_{90}}\sin^4\theta} \quad (6)$$

where, E_0 and E_{90} are Young's moduli in the direction parallel and normal to the bed joints respectively; $\nu_{0\text{-}90}$ is Poisson's Ratio defined as the ratio of the strain in the direction normal to the bed joints due to the strain in the direction parallel to the bed joints; and G is the shear modulus.

It is common to relate the initial Young's modulus of quasi-brittle materials such as concrete and masonry to their ultimate compressive strength. Therefore it seems rational to assume that, not only Young's modulus will change, but also the ultimate strength of the masonry panel in the θ direction, $f'_{m\text{-}\theta}$. A simple way to account for this direction variation is to relate E_θ to $f'_{m\text{-}\theta}$ using the same factor relating E_{90} to $f'_{m\text{-}90}$ and neglect the shear stress effect, since the infill is failing in a *CC* mode, as well as the effect of the biaxial state of stress in the infill corners vicinity. The reason for choosing E_{90} and $f'_{m\text{-}90}$ is that it is a common practice as well as a standard test (*ASTM E-447*), to obtain the strength of masonry prisms in a direction perpendicular to bed joints i.e. the vertical direction, which is usually the loading direction in load-bearing walls. The assumption that the masonry compressive strength varies according to the angle of loading was investigated by Hamid and Drysdale (1980) and a value of $f'_{m\text{-}0} = 0.7\, f'_{m\text{-}90}$ was suggested by Seah (1998). Fig. 6-a shows the orthotropic model for the masonry panel.

Based on non-linear FE analyses, Saneinejad and Hobbs (1995) suggested that the *secant stiffness* of the *infilled frames* at the peak load to be half the *initial stiffness*. This might be directly interpreted into the stress strain relation for the masonry panel by assuming that the *secant Young's modulus* at peak load E_p is equal to half the *initial Young's modulus*, E_θ, i.e. $E_p = 0.5\, E_\theta$ .This assumption is justified since the stiffness of the *infilled frame* is affected primarily by the stiffness of the *infill* [Dhanasekar and Page (1986)].

As shown in Fig. 6-b knowing E_p and f_θ , it is now an easy task to determine the strain corresponding to the peak load ε_p . Instead of using the *parabolic* stress-strain relation shown in Fig. 6-b, it is suggested to approximate it into a *tri-linear* relation which is simpler and more practical for analysis as shown by the thick lines in the same figure. Unless more accurate data are available, the parameters in Fig. 6-b will be assumed according to the following

$$\varepsilon_1 = \varepsilon_p - 0.001 \qquad \varepsilon_2 = \varepsilon_p + 0.001 \qquad \varepsilon_u = 0.01 \quad (7\text{-a,b,c})$$

Knowing the stress strain relation along with the area (from equation 5) and the length of each of the three struts (which can be easily calculated knowing the panel dimensions and the contact lengths given by equations 3-a and 3-b) makes it possible to obtain a *force-deformation* relation for each strut. As shown in Fig. 6-c, by simply multiplying the strains ε_1, ε_2 and ε_u by the length of each strut resulting in obtaining δ_1, δ_2 and δ_u respectively. Also multiplying the stress, $f'_{m\text{-}\theta}$, by the area of each strut results in obtaining F_u for each strut. In fact assuming that E_θ and $f'_{m\text{-}\theta}$ are the same for all struts and neglecting the minor difference

in the inclination angle between the middle strut and both the upper and the lower strut, will result in finding only two distinct force-deformation relations, one for the upper and lower struts and another for the middle strut.
It is worth mentioning that, the use of a macro model, that is neither a single strut, nor a plate to represent the panel was previously suggested by some researchers. Chrysotomou (1991) and Mander and Nair (1994) suggested multiple strut models. Mosalam et al. (1997c) used a truss with contact elements. Due to the complexity of the problem, most of the properties of these macro models suggested by different researchers were not justified based on the *material level*, unlike the suggested model. In fact, the areas and the stiffnesses of the members representing the panel were generally selected to *match* either some experimental findings like the stiffness and/or the ultimate load or the natural frequency under seismic loading. In other cases the properties of the macro model were selected merely to match some properties of a more sophisticated micro model.

MODELING OF TEST SPECIMENS USING THE PROPOSED METHOD

The suggested method was used to model three CMISF specimens. Two of the specimens were tested at the University of New Brunswick under monotonic racking load by Yong (1984) and Richardson (1986) and the third was tested in Cornell University by Mosalam et al. (1997a) under quasi-static displacement. The first two specimens are identical single panel CMISF with different masonry strength. The reasons for choosing these specimens are primarily for the experimental results consistency as well as to verify the effect of changing the masonry strength on the CMISF model behavior, and because these experimental results were duplicated by Seah (1998) using a very sophisticated *micro* FE model consisting of series of plane stress elements connected by ten springs at each node. The third specimen is a one fourth scale, two bay-single story CMISF with semi-rigid connection, this specimen was chosen to demonstrate the effectiveness of the method to model semi-rigid connections and the effect of using three struts on changing the bending moment diagram of CMISF. The details of the calculations involved in the FE modeling of these specimens can be found elsewhere [ElDakhakhni (2000)].

The ANSYS®5.3 FE program was used to generate the load-deflection relation of specimen WB2 tested by Yong (1984), utilizing the proposed technique. The load-deflection relations for the bare and the infilled frame model are shown in Fig. 7-a along with test results for comparison. It is worth mentioning that the specimen was loaded until the lateral displacement reached approximately 20 mm at which it was assumed that the specimen failed. It might be noted that a sudden drop of the load-deflection curve occurred at approximately 312.0 kN. This was due to the development of the *diagonal crack* discussed earlier. The developing of the diagonal crack affects neither the stiffness nor the ultimate load capacity of the infilled frame and it will result only in a sudden drift, affecting the overall ductility of the system, which is outside the scope of this study. The figure shows the capabilities of the proposed method to predict both the stiffness and ultimate load capacity up to failure. The model appears to overestimate the ultimate capacity by about 9% and acceptably estimates the average stiffness up to failure.

Another specimen WD7, tested by Richardson (1986), was modeled using the same technique utilizing the ANSYS®5.3 FE program and the load-deflection relations for the bare and the infilled frame model are shown in Fig. 7-b along with test results for comparison. Again the proposed model is efficient in duplicating the test results up to failure. The model underestimated the failure load by 10% and the experimental test data show that the infilled frame gradually degrades and eventually at some point it will reach the ultimate capacity of the bare frame.
It is worth mentioning that the proposed model can predict the stiffness and strength efficiently up to failure, yet the post peak behavior and the ductility of CMISF systems are highly uncertain and will require further research, currently being undertaken by the authors at Drexel University.

Specimen Q21SSB, tested by Mosalam et al. (1997a) was modeled using the same technique; Fig. 8-a show the load-deflection relation of the bare frame model and the infilled frame model along with envelope of the cycling loading test after correcting it to exclude the effect of the lack of fit between the frame and the infill. The model accurately represents the infilled frame up to a deflection of 6 mm, at which the model underestimated the specimen capacity by less than 2%. After this displacement, failure occurred in the specimen yet the model continued to carry more load, but with a very low stiffness, then it gradually loses its strength and fails. Fig. 8-b shows the bending moments in the model members at a load of 41.5 kN, before failure. These moments have the same trend as those obtained by Mosalam et al. (1997b) and suggested by Reflak and Fajfar (1991), Saneinejad and Hobbs (1995), Buonopane and White (1999), and Furutani et al. (2000).

CONCLUSIONS

This paper presents an analytical method of predicting the stiffness and the ultimate load capacity of CMISF failing in *CC* mode. Based on the present study, the following conclusions can be inferred:

1. The proposed analytical technique predicts the lateral stiffness up to failure, and the ultimate load capacity of concrete masonry-infilled steel frames (CMISF) to an acceptable degree of accuracy. The technique accounts for the nonlinear behavior that occurs in both the steel frame due to formation of plastic hinges, and in the masonry panel due to crushing. The technique considers the diagonal tension cracking in the masonry joints merely as a serviceability limit state.
2. The use of three struts instead of a single one is justified based on the observed bending moments in the frame members, which cannot be generated using a single strut. Furthermore, the three struts do not fail *simultaneously*, which is the case in actual infill panels, since the crushing *starts* at the corners and keeps *propagating* in the corner *region* leading to failure of the panel. The use of the three struts will also facilitate modeling the *interaction* between the different panels in multi-story buildings.

3. The technique presents a *macro-model* that is more easy and practical to apply and require much less time than techniques based on treating the panel as a plate, *meso-models*, or descretizing the panel as a series of plane stress elements interconnected by a series of springs or contact elements, *micro-models*.
4. In order to use this technique in actual multi-story, multi-bay frame structures, three diagonal struts should replace each infill panel following the steps of the proposed method. This process can be easily computerized and included into the FE programs used in structural analysis in order to automatically generate the diagonal struts and place them in their proper locations with their respective properties.
5. Instead of using the actual nonlinear stress-strain relation, an option, which might not be available in many structural analysis software, a simplified tri-linear stress-strain relation is employed for the masonry. A similar relation is also used in modeling the steel frame load-deformation relation. It is worth mentioning that this simplification results in a less solution time, specially, in multi-story 3-D structures with large number of DOF.

ACKNOWLEDGEMENTS

The work presented herein is part of a study performed at Drexel University under Grant No. CMS-9730646 from the National Science Foundation (NSF); Dr. Shih-Chi Liu is the NSF program director for this research. The results, opinions, and conclusions expressed in this paper are solely those of the authors and do not necessarily reflect those of the NSF.

REFERENCES

American Society for Testing and Materials, ASTM E 447-92b, "Standard Test Methods for Compressive Strength of Masonry Prisms," Annual Book of ASTM Standards, Vol. 04.05, West Conshohocken, PA.

American Society for Testing and Materials, ASTM E 519-81, "Standard Test Method for Diagonal Tension (Shear) in Masonry Assemblages," Annual Book of ASTM Standards, Vol. 04.05, West Conshohocken, PA.

ANSYS®5.3, ANSYS® Inc. 201 Johnson Road, Houston, PA 15342-1300.

Buonopane, S. G., and White, R. N., 1999. "Pseudodynamic testing of masonry infilled reinforced concrete frame", ASCE Journal of Structural Engineering, Vol. 125, No. 6, pp. 578-589

Chrysostomou, C. Z., 1991. "Effect of degrading infill walls on the nonlinear seismic response of two-dimensional steel frames", Ph.D. thesis , Cornell University, Ithaca, NY, 1991.

Chen, W. F., and Lui, E. M., 1991. "Stability Design of Steel Frames", CRC Press.

Dhanasekar, M., and Page, A. W., 1986. "The influence of brick masonry infill properties on the behavior of infilled frames", Proceedings of the Institution of Civil Engineers, Part 2, Vol. 81, pp. 593-605.

Drysdale, R. G., and Hamid, A. A., 1979. "Behavior of concrete block masonry under axial compression", ACI Journal. Vol. 76, pp. 707-721.

ElDakhakhni, W. W. (2000) “Non-Linear Finite Element Modeling of Concrete Masonry-Infilled Steel Frame,” M.Sc. thesis, Drexel University, Philadelphia, PA, 19104.

Flanagan, R. D., Bennett, R. M., and Barclay, G. A., 1992. “Experimental testing of hollow clay tile infilled frames”, Proceedings, 6th. Canadian Masonry Symposium, University of Saskatchewan, Saskatchewan, Canada. pp. 633-644.

Flanagan, R. D., Bennett, R. M., and Barclay, G. A., 1999. “In-plane behavior of structural clay tile infilled frames”, ASCE Journal of Structural Engineering, Vol. 125, No. 6, pp. 590-599.

Furutani, M., Imai, H., and Matsumoto, T., 2000. “12th World Conference on Earthquake Engineering”, Auckland, New Zealand, February 2000, on CD-ROM.

Hamid, A. A. and Drysdale, R. G., 1980. “Concrete masonry under combined shear and compression along the mortar joints”, ACI Journal. Vol. 77, pp. 314-320.

Khattab, M. ,and Drysdale, R. G. 1992. “Test of concrete block masonry under biaxial tension-compression”, Proceedings, 6th. Canadian Masonry Symposium, University of Saskatchewan, Saskatchewan, Canada. pp. 645-656.

Liauw, T. C., and Kwan, K. H., 1982. “Non-linear analysis of multi-storey infilled frames”, Proceedings of the Institution of Civil Engineers, Part 2, Vol. 73, pp. 441-454.

Mander, J.B and Nair, B. 1994. Seismic resistance of brick-infilled steel frames with and without retrofit. TMS journal February 1994. pp. 24-37.

McBride, R. T., 1984. “The behavior of masonry infilled steel frames subjected to racking”, M.Sc. thesis, Department of Civil Engineering, University of New Brunswick, Fredericton, NB, Canada.

Mosalam, K., White, R. N., and Gergely, P., 1997a. “Seismic Evaluation of Frames with Infill Walls Using Quasi-static Experiments”. Technical report NCEER-97-0019.

Mosalam, K., White, R. N., and Gergely, P., 1997b. “Seismic Evaluation of Frames with Infill Walls Using Pseudo-dynamic Experiments”. Technical report NCEER-97-0020.

Mosalam, K., White, R. N., and Gergely, P., 1997c. “Computational Strategies for Frames with Infill Walls: Discrete and Smeared Crack Analyses and Seismic Fragility”. Technical report NCEER-97-0021.

Polyakov, S. V., 1956. “Masonry in framed buildings (Godsudarstvenoe Isdatel' stvo Literatury Po Stroidal stvui Architecture. Moscow, 1956). Translated by G. L. Cairns in 1963.

Richardson, J., 1986. “The behavior of masonry infilled steel frames”. M.Sc. thesis, University of New Brunswick, Fredericton, NB, Canada.

Saneinejad A., and Hobbs, B., 1995. “Inelastic design of infilled frames”. ASCE Journal of Structural Division, Vol. 121, No. ST4, pp. 634-650.

Seah, C. K. 1998. “A universal approach for the analysis and design of masonry infilled frame structures” Ph.D. Thesis, University of New Brunswick, Fredericton, NB., Canada.

Shames, I. H., and Cozzarelli, F. A., 1992. “Elastic and Inelastic Stress Analysis”, Prentice Hall , Englewood Cliffs, New Jersey 07632.

Stafford Smith, B., and Carter, C., 1969. “A method of analysis for infilled frames”. Proceedings, the Institution of Civil Engineers, Vol. 44, pp. 31-48.

Yong, T. C., 1984. "Shear strength of masonry panels in steel frames". M.Sc. thesis, University of New Brunswick, Fredericton, NB, Canada.

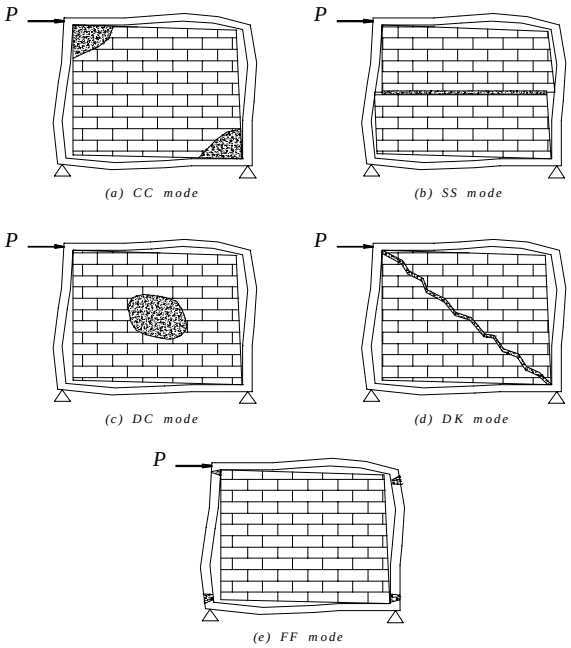

Figure 1. Different Failure Modes of Masonry Infilled Frames:
(a) *C*orner *C*rushing Mode; (b) *S*liding *S*hear Mode; (c) *D*iagonal *C*ompression Mode
(d) *D*iagonal Crac*k*ing Mode; (e) *F*rame *F*ailure Mode

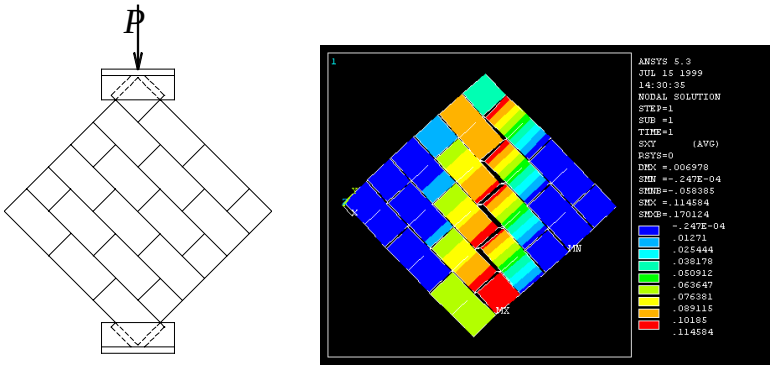

(a) (b)

Figure 2. The Diagonal Tension Specimen : (a) *ASTM E-519*Test Setup; (b) Shear Stress Contours and Failure Mode Obtained Using The ANSYS®5.3 FE Model

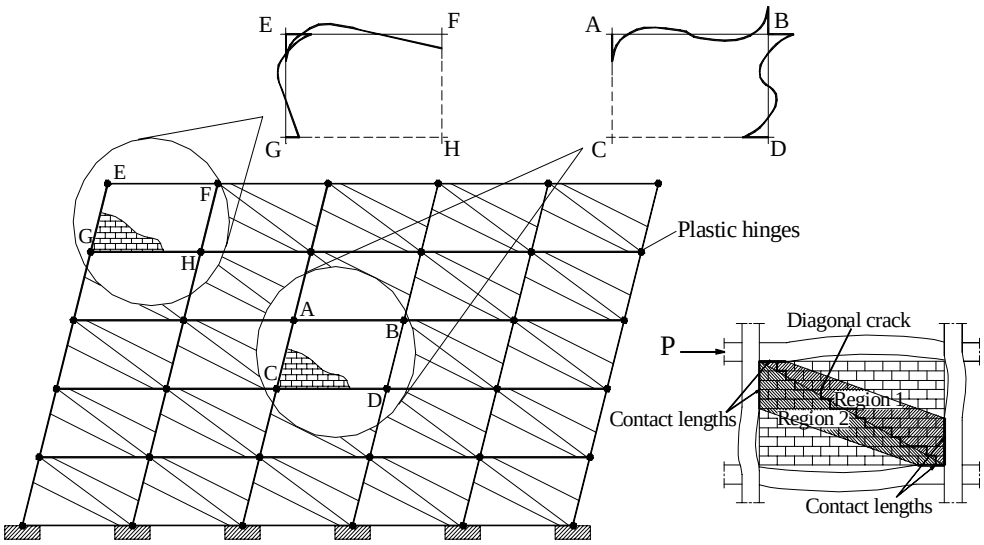

Figure 3. The Infill Panel Separation into Two Diagonal Regions, and The Resulting Bending Moment Diagrams for a Different Bays in Multi-Story Infilled Frame Building

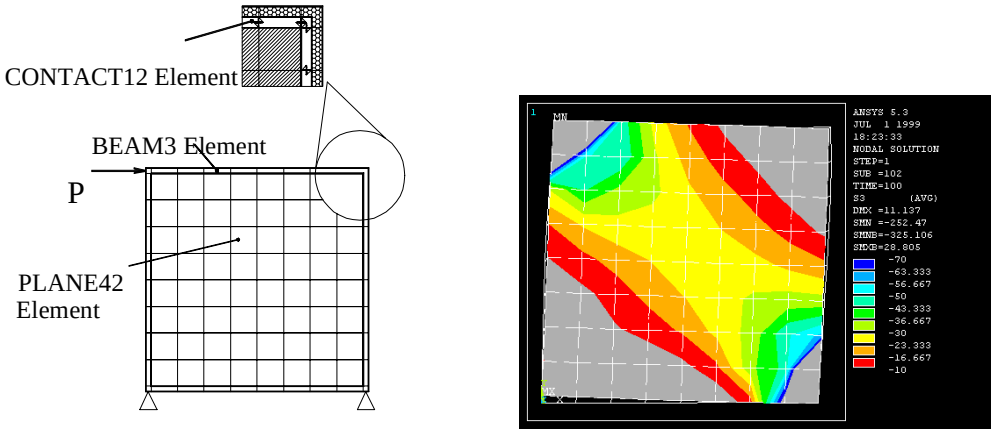

(a) (b)

Figure 4. ANSYS®5.3 FE Model of a Single panel Infilled Frame: (a) Schematic Diagram; (b) Principal Stress Contours

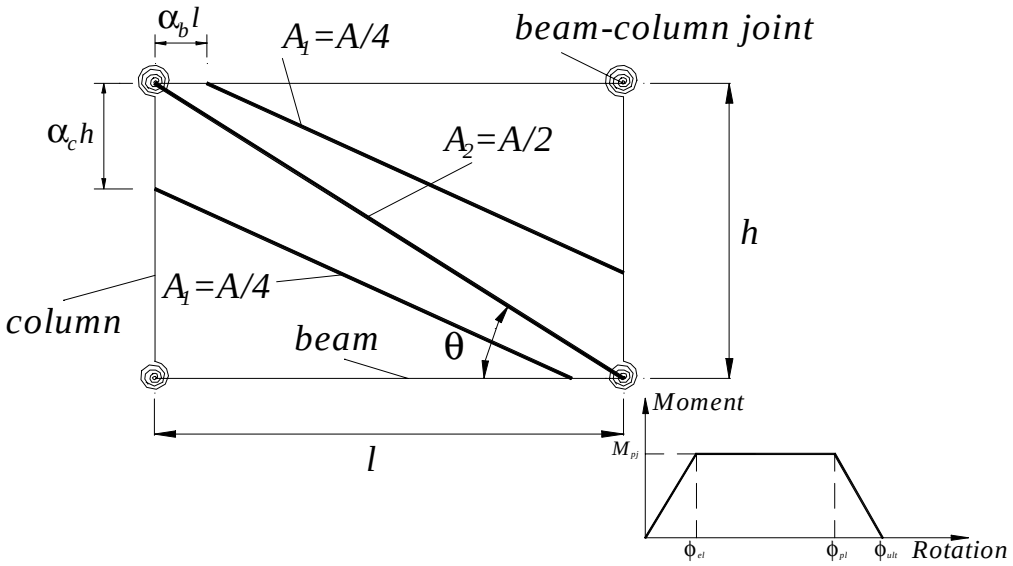

Figure 5. The Proposed CMISF Model and The Beam-Column Connection Behavior

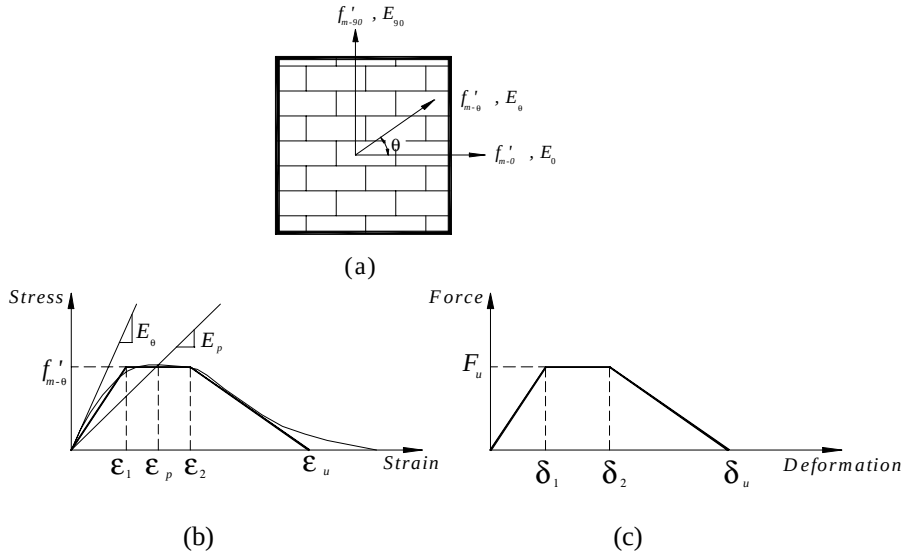

Figure 6. Concrete Masonry Behavior : (a) Orthotropic Model
(b) Tri-Linear Stress-Strain Relation; (c) Typical Force-Deformation Relation for Struts

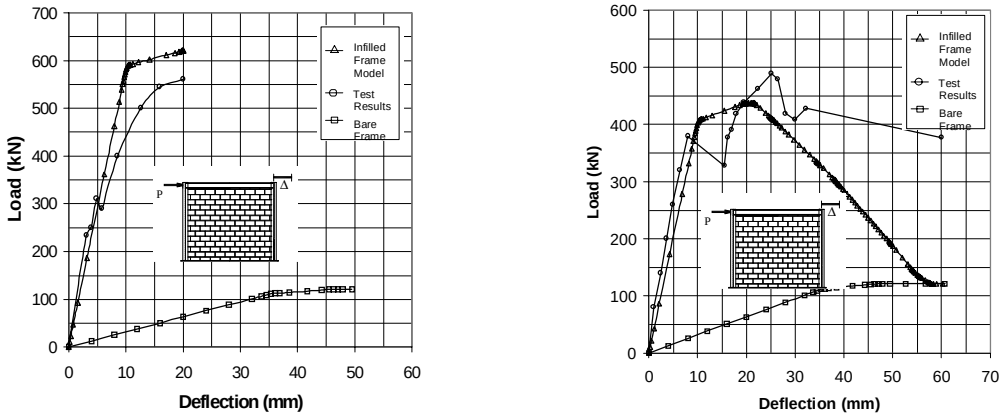

(a) (b)

Figure 7. Load-Deflection Relations for Specimen : (a) WB2, (b) WD7

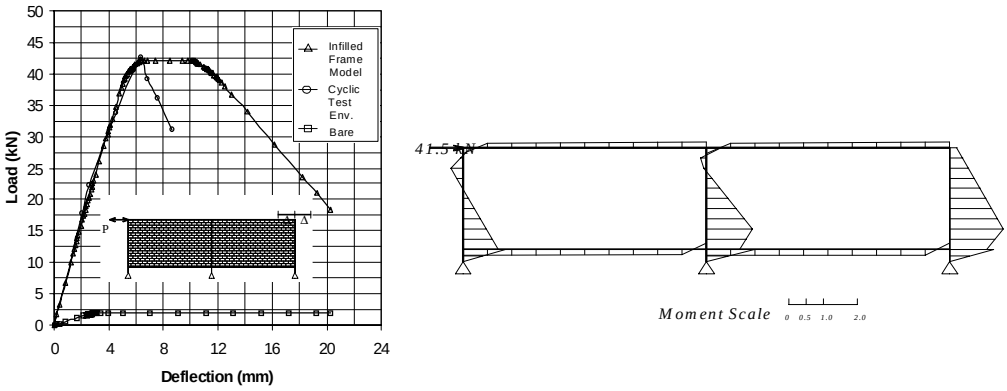

(a) (b)

Figure 8. Specimen Q21SSB : (a) Load-Deflection Relations, (b) Bending Moment Diagram obtained using ANSYS®5.3 (drawn on the tension side)